

# HiPR-FISH spatial mapping of cheese rind microbial communities

Seeing how microbes are organized within a community can inspire hypotheses about how species interact with each other. We used HiPR-FISH spatial imaging to look at the distribution of microbes within five distinct microbial communities growing on the surface of aged cheeses.

## Contributors (A-Z)

Rachel J. Dutton, Megan L. Hochstrasser, Taylor Reiter, Emily C.P. Weiss

*Version 1 · Mar 31, 2025*

## Purpose

Understanding how microbes organize spatially within a community can tell us a lot about microbial ecology. Visualizing this organization in dense and complex microbial communities has previously posed a technical challenge.

We applied a recently published technique for spatial imaging of biofilms, HiPR-FISH, to cheese rind microbiomes to evaluate its use for generating hypotheses about the microbial ecology of this system. We've paired this imaging data with metagenomic sequencing data.

We hope that this collection of resources will be useful to microbiome researchers interested in applying spatial imaging techniques to their system or in developing tools to integrate paired datasets.

- **Spatial imaging data** from this pub is available on [Zenodo](#).
- The **code** we used to create the [Figure 5](#) heatmap is available in [this GitHub repository](#).
- We applied metagenomic sequencing [\[1\]](#) to the same cheese communities that we used for spatial analysis in this pub. You can find **raw sequencing and assembly data** on the [European Nucleotide Archive](#).

## Background and goals

When studying the interactions between microbes and their environment, we often use metagenomic or metatranscriptomic sequencing to determine which microbes are present and assess their functional capabilities. However, these techniques do not tell us anything about the spatial organization of microbes within the microbial community. Understanding these spatial relationships is important for understanding the true context of microbial life within the community. Spatial information can also be useful for generating hypotheses about how microbes interact with other organisms and with abiotic factors.

HiPR-FISH, or high-phylogenetic-resolution microbiome mapping by fluorescence *in situ* hybridization, is a technique for creating visual maps that show where microorganisms live within complex community biofilms at single-cell resolution [\[2\]](#). This technique, which researchers initially applied to mouse gut and human oral plaque microbiomes, uses combinatorial fluorescent labeling to distinguish hundreds of species of microorganisms in a single sample [\[2\]](#).

Cheese rind microbial communities are a validated experimental system for studying microbial ecology [\[3\]\[4\]\[5\]\[6\]](#). When we began the efforts described here, we hoped to gather multiple types of rich data about cheese rind communities [\[1\]](#) for downstream biological discovery. Though it had not yet been applied for this type of

microbiome, we were intrigued by HiPR-FISH, so we decided to see how it performed across several cheeses. We wanted to determine whether this approach could provide useful information and help us generate hypotheses about interspecies interactions.

**SHOW ME THE DATA:** Access our [spatial imaging data](#).

# The approach

HiPR-FISH is a new technique that requires sample preparation and probe design expertise that we don't have in-house, so we contracted with [Kanvas Biosciences](#) for this work. We collected cheese rind samples and sent them to Kanvas, where scientists carried out FISH probe creation, sample processing, imaging, image processing, and data analysis as part of their HiPR-Map service. Aside from "Sample collection" and part of the "Probe design" subsection below, Kanvas provided the remainder of the methodological descriptions we've included here.

## Sample collection

During a large-scale collection effort of cheese rind microbiome samples [1], we collected small sections of intact cheese rinds from five different washed-rind cheeses (Table 1), as described [here](#). Although we had time-series samples available, we decided to prioritize testing multiple cheeses rather than time points of the same cheese; we hoped this would help us better evaluate how this technique works across different communities. After harvesting, we immediately stored sections at  $-80^{\circ}\text{C}$  prior to shipping to [Kanvas Biosciences](#) on dry ice. We initially tried fixing the sections of cheese in PFA rather than freezing fresh samples, but this seemed to cause some of the rinds to dissolve.

Cheese	Age of collected sample	Full aging time of cheese
EL	1 month	2–3 months
OM	1 month	2.5–3.5 months
WI	3 weeks	1.5–3 months

Cheese	Age of collected sample	Full aging time of cheese
AL	4 months	8–12 months
WH	2 months	3–6 months

**Table 1. Information about the cheese samples we used in this study.**

## Probe design

We used metagenomic assemblies from Oxford Nanopore Technologies sequencing data from the rind communities from the same cheese wheels we sampled here (available in the [European Nucleotide Archive](#) as assemblies ERZ15415241, ERZ15415243, ERZ15614078, ERZ15271657, and ERZ15271649) to predict 16S and 18S ribosomal RNA sequences for use in spatial imaging probe design. We concatenated assemblies from these five cheeses together to make a master assembly so that we could design one HiPR-FISH probe pool that would work for all five cheeses. We then used [Barrnap](#) v0.9 to predict ribosomal sequences from the master assembly using the `kingdom` options for eukaryotes, bacteria, and archaea. Since we can sometimes miss ribosomal regions in metagenomic assemblies, we also wanted to do prediction directly from the ONT sequencing reads. We concatenated ONT reads from the sequencing of all five cheeses (also available on the [ENA](#)) into one FASTQ file and mapped this back to the master assembly using minimap v2.22-r1101 [7][8]. We then extracted unmapped reads to a new file using SAMtools v1.9 with HTSlib v1.9 [9][10]. We did the same Barrnap prediction for the unmapped reads. We only recovered one new bacterial 16S gene from the unmapped reads and added this sequence to the predictions from the master assembly. We then used CD-HIT-EST v4.8.1 with a sequence identity threshold of one to cluster the combined assembly and unmapped read predictions. This clustering resulted in a total of 141 predicted 16S/18S sequences. We provided these sequences to Kanvas Biosciences for probe creation.

Kanvas Biosciences grouped FASTA sequences in similar taxa by sequence similarity of amplicon sequence variants (ASVs). For each of the 53 identified ASVs, they selected different probe sequences with high specificity and concatenated with landing pads corresponding to secondary fluorescent readout oligos [2]. Taxa assignments are provided as species assigned by alignment to reference databases

and followed by a number if there are multiple distinct groups whose closest relatives in the reference database correspond to the same species.

## Sample processing

Kanvas Biosciences received frozen cheese core specimens from Arcadia Science. Their scientists embedded cores in OCT, froze them in liquid nitrogen, and stored them at  $-80^{\circ}\text{C}$ . They sectioned the cheese cores at a thickness of 2–4  $\mu\text{m}$  using a cryotome and placed them on Ultrastick slides with rind orientation marked. For the hard cheeses (AL and WH), they noted a waxy residue and required short heating (to  $75^{\circ}\text{C}$ ) and annealing (on ice) to secure sections to the slide. They fixed cheese sections in 2% formaldehyde for 90 minutes and stored in 70% ethanol until performing the HiPR-FISH assay. They included probes that target Eubacterium and pan-fungal rRNA in addition to the custom probe pool (target sequences: Eub =  $\text{*GCTGCCTCCCGTAGGAGT*}$ , PF =  $\text{*CTCTGGCTTCACCCTATTC*}$ ); asterisks represent proprietary sequences that bind the readout probes.

## Imaging and image processing

Scientists at Kanvas Biosciences imaged specimens on a Zeiss i880 confocal in spectral mode. For each specimen, they collected seven fields of view, each with a size of  $135\ \mu\text{m} \times 135\ \mu\text{m}$ . They collected spectral data using multiple laser excitations between 405 nm and 633 nm, generating emission spectra between 405 nm and 680 nm. Following image collection on the confocal, they imaged sections with a tile scan on a Zeiss widefield epifluorescence microscope to determine the relative positions of confocal fields of view. They processed images using Kanvas' proprietary software. Briefly, they segmented each microbe to determine cell boundaries. They compared the spectra within the boundaries of each segmented object to Kanvas' database to perform barcode identification and provide quality metrics.

# Data analysis and deposition

The **code** we used to create the [Figure 5](#) heatmap is available in [this GitHub repository](#) (DOI: [10.5281/zenodo.7853296](#)).

Kanvas conducted several analyses to quantify microbial abundance and interactions in cheese rinds. For each field of view (FOV), their team calculated the abundance of each amplicon sequence variant (ASV) and determined the Pearson correlation between FOVs. Kanvas Biosciences also evaluated spatial proximity between microbes by constructing a region adjacency graph based on distance ( $\leq 5$  microns) and calculating the total number of edges between taxa. To assess taxa enrichment, they compared the observed spatial association matrix to 250 random matrices using fold-change and a t-test, with p-values corrected by Bonferroni. Random matrices are constructed by randomly scrambling the detected barcode in a field of view among segmented objects and then measuring the spatial association matrix. Taxonomic assignments are based on NCBI nucleotide BLAST [11] matches of the ribosomal sequences used for probe design, and are therefore tentative.

We uploaded all of the resulting data to [Zenodo](#) (DOI: [10.5281/zenodo.7613703](#)).

## The results

**SHOW ME THE DATA:** Access our [spatial imaging data](#).

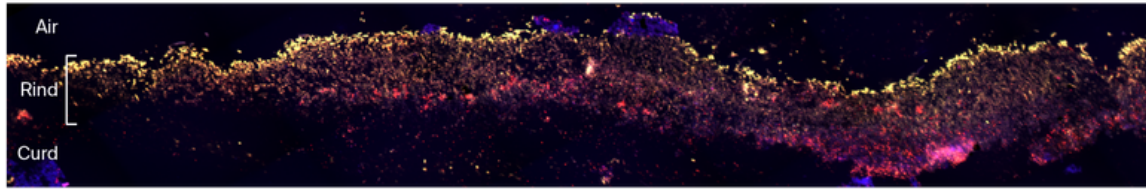


**Figure 1**

**WI sample rind labeled with eubacterial and panfungal probes.**

Bacteria are displayed in red and fungi are displayed in yellow. The top of the image is the outermost part of the rind/cheese exterior, whereas the bottom of the image below the red bacteria is the interior of the cheese/cheese curd. We adjusted this image to increase brightness and contrast. Purple coloring is background fluorescence and does not represent a biological signal.

ARC1\_WI\_WF\_overlay.png is a zoomed-out version of this image, which you can find in the full data available on [Zenodo](#).

The rinds that form on the surface of aged cheeses are dense microbial biofilms made up of viruses, bacteria, and fungi. We used spatial imaging to look at the spatial organization of microbes within five different cheeses. Using generic probes, we were able to detect both bacteria and fungi within the rind. For our WI cheese sample, it seems that bacteria are concentrated close to the cheese curd, whereas fungi are concentrated on top of the bacteria in the outermost layer of the rind ([Figure 1](#)).



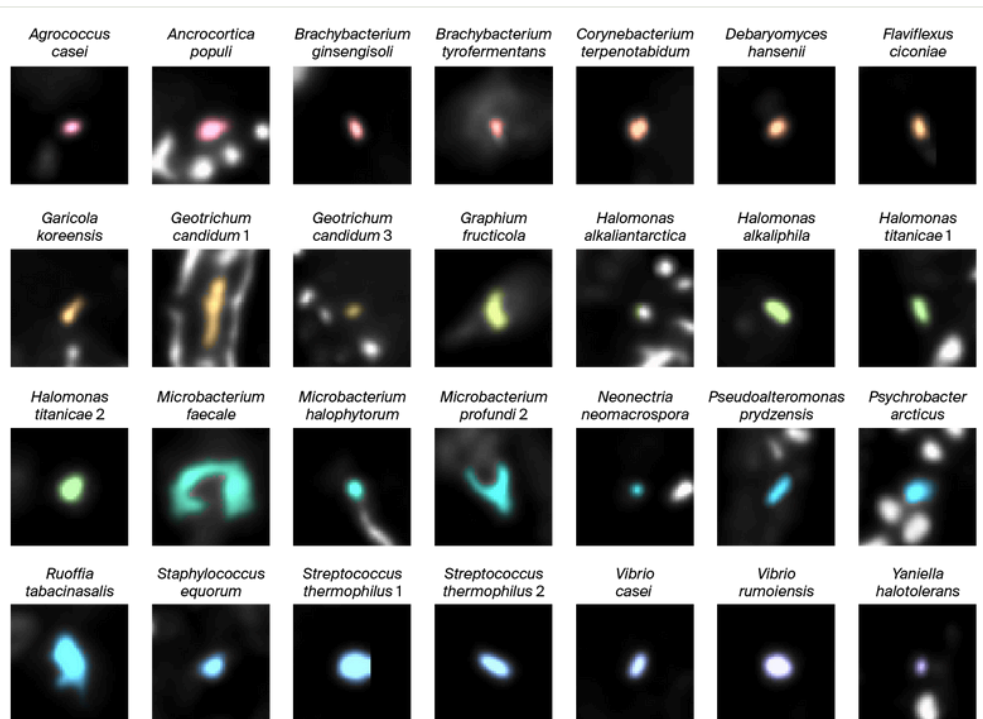


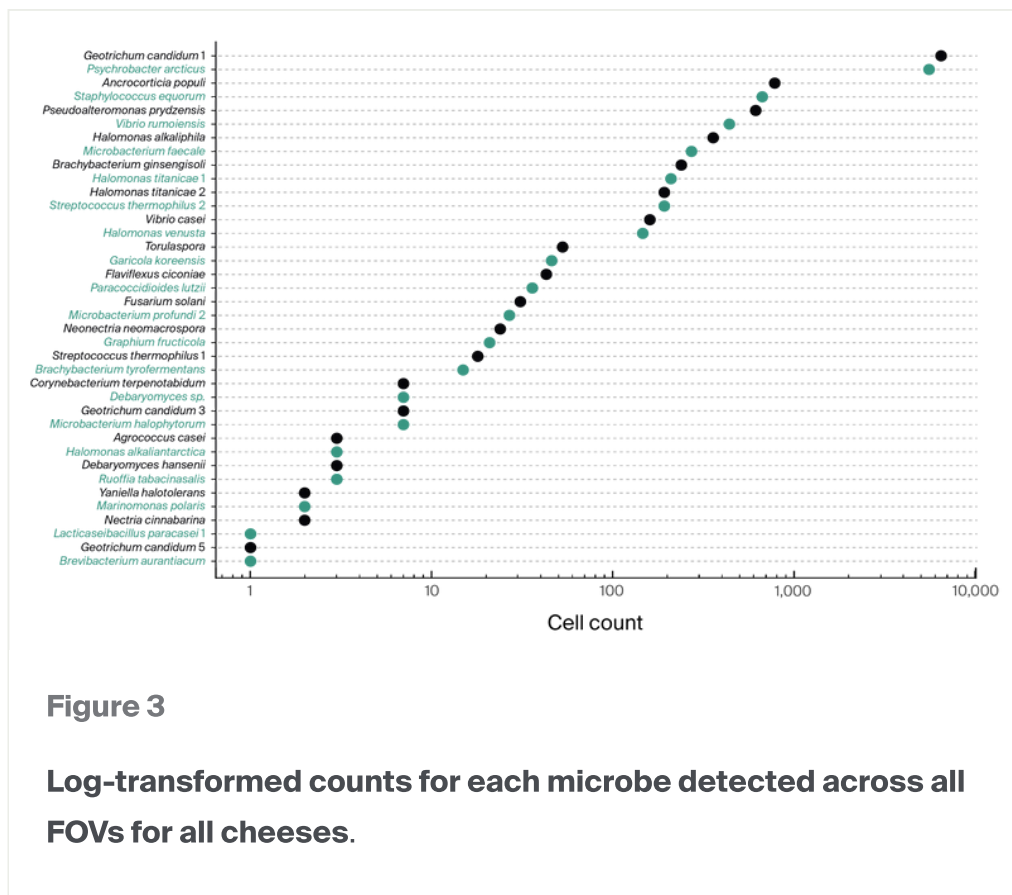
**Figure 2**

**Example images of single cells of 28 of the predicted amplicon sequence variants that we detected by HiPR-FISH, with false coloring to highlight the cell of interest.**

All images are at the same scale. The morphologies depend on the orientation of the microbe in the focal plane, how close it is to neighboring cells, the distribution of rRNA within the cells, and other factors – interpret cautiously.

We designed HiPR-FISH probes, which enable the specific identification of many microbial species at high spatial resolution, for five cheese rinds based on ribosomal sequences predicted from metagenomic sequencing data [1]. Using the master probe panel we designed against these five cheeses, we were able to detect 38 out of the 53 amplicon sequence variants (ASVs) that we targeted (Figure 2).





The species we detected included both bacteria and fungi (*Debaryomyces* and *Geotrichum*). We attributed the majority of detected microbes to *Geotrichum* and *Psychrobacter* (Figure 3 and Figure 4), which is consistent with the high abundance of these microbes in the EL and OM communities based on Illumina sequencing data [1].

Overall, the detected species and their relative abundances was mostly consistent with our metagenomic sequencing data, with the exception of the actinomycete *Ancrocarticia populi*. For *A. populi*, we identified cells using a combination of probes that we later determined to be spectrally similar to autofluorescent droplets found in cheese samples. It is possible that some segmented objects classified as *A. populi* were in fact autofluorescent droplets, skewing our abundance estimates. Where possible, Kanvas performed manual segmentation to exclude droplets from downstream analyses. It is also possible that the taxonomic assignment is inaccurate, although the metagenomic contig that we pulled the *A. populi* 16S sequence from does appear to belong to an actinomycete.

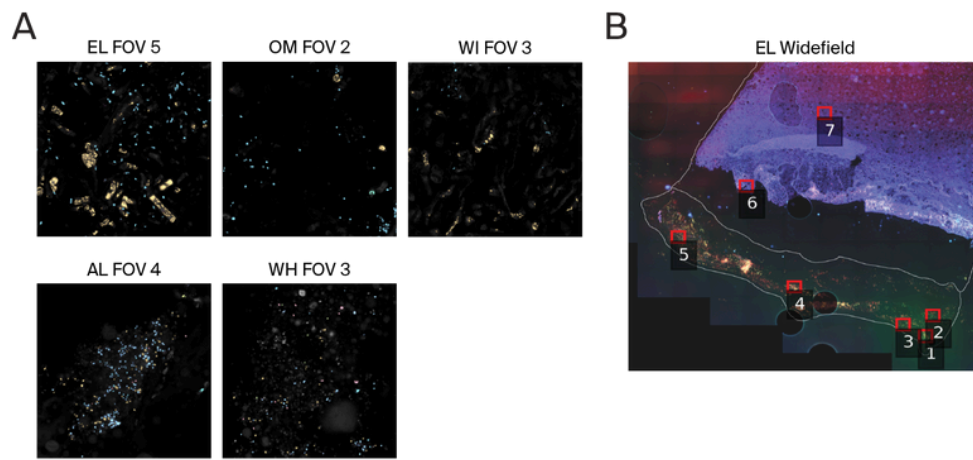


**Figure 4**

**Example fields of view (FOVs) for each of the five cheeses (A) and an example corresponding widefield image for EL with FOVs mapped on the image (B).**

FOVs are 75  $\mu\text{m}$   $\times$  75  $\mu\text{m}$ .

Kanvas Biosciences also performed correlation analysis to look for consistent positive or negative associations between microbes ([Figure 5](#)). They then did taxa enrichment analysis, on a per-cheese basis and across the whole dataset, to compare these spatial associations of microbes to what might be observed by chance. However, only one negative association was significant (*Geotrichum candidum* 1 and *Ancrocorticia populi*). This is likely to be a false positive rather than a true indication of microbial interaction, as these species do not often exist in the same images or at similar concentrations in those images.

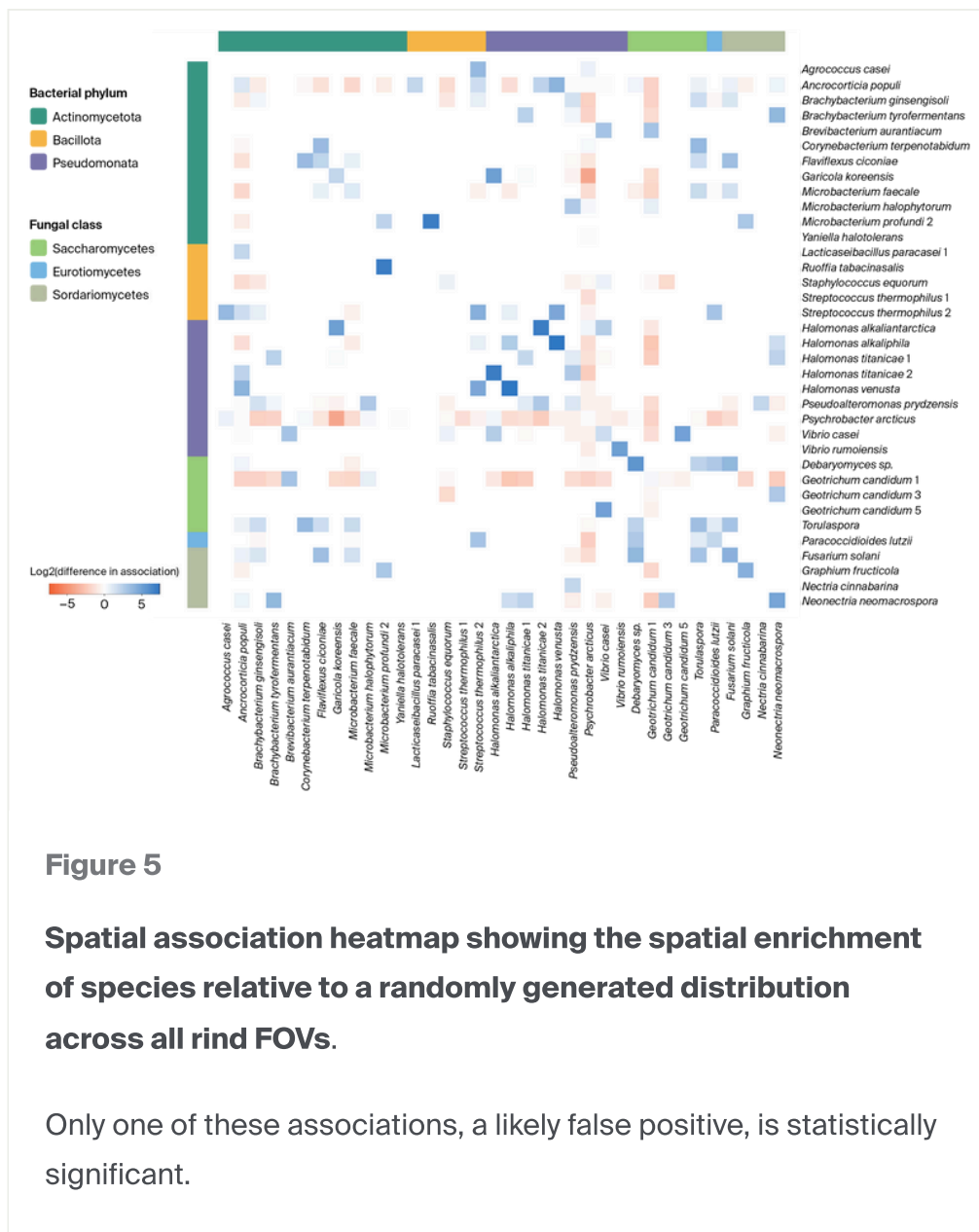


**Figure 5**

**Spatial association heatmap showing the spatial enrichment of species relative to a randomly generated distribution across all rind FOVs.**

Only one of these associations, a likely false positive, is statistically significant.

Overall, there were many microbial cells for which we could not detect sufficient fluorescent signal due to low ribosomal density, which in turn may have led to a lack of significant spatial associations. For example, cells closer to the cheese curd had lower signals from both Eubacterium/pan-fungal probes and the ASV-specific panel, perhaps indicating that cells there are less metabolically active. During imaging, it was technically challenging to detect cells with low signal while also avoiding oversaturation of brighter cells. Although we designed probes for filamentous fungi such as *Fusarium* and *Scopulariopsis*, which we detected in our metagenomic sequencing data, we were not able to detect these species using HiPR-FISH, perhaps because of challenges of getting probes through the cell walls of these organisms. While we do not expect that it is the major cause of cells without probe signal, probe

design from PacBio sequencing data (which is normally used for HiPR-FISH) may have been more successful than the prediction from ONT data that we used here.

The full data set, which is available on [Zenodo](#), includes the following:

- For each field of view (roughly 135  $\mu\text{m}$   $\times$  135  $\mu\text{m}$ ; 7 FOVs per each cheese specimen):
  - A fluorescence intensity image (\*\_spectral\_max\_projection.png/.tif).
  - A pseudo-colored microbe-labeled image (\*\_identification.png/.tif).
  - A data frame contains each identified microbe's identity, position, and size (\*\_cell\_information.csv).
  - A segmented mask for microbiota (\*\_segmentation.png/.tif)
  - A spatial proximity graph for each species close to each other, showing the spatial enrichment over random distribution (\*\_spatialheatmap.png).
  - A corresponding dataframe used to generate the spatial proximity graph (\*\_absolute\_spatial\_association.csv) and dataframe for the average of 500 random shuffles of the taxa (\*\_randomized\_spatial\_association\_matrix.csv).
- For each cheese specimen:
  - A widefield image with FOVs located on the image (\*\_WF\_overlay.png).
- In general:
  - A PNG showing the color legend for each species. (ARC1\_taxa\_color\_legend.png)
  - A data frame showing the environmental location of each FOV in the cheese (RIND/CURD) and the location of each FOV relative to FOV 1. (ARC1\_Cheese\_Map.csv).
  - A vignette showing ASV false-coloring according to its taxonomic identification (ARC1\_detected\_species\_representative\_cell\_vignette.png).
  - Sequences used as input in probe design (16S\_18S\_forKanvas.fasta).
  - A CSV file containing the sequences that belong to each ASV (ARC1\_sequences\_to\_ASVs.csv).
  - Plots of log-transformed counts for each microbe detected across all FOVs, and broken down for each cheese (\*detected\_species\_absolute\_abundance.png).
  - CSVs containing pairwise correlation of FOVs based on spatial association (ARC1\_spatial\_association\_FOV\_correlation.csv) and microbial abundance

(ARC1\_abundance\_FOV\_correlation.csv).

- Plots of spatial association matrices, aggregated for different cheeses and different locations (RIND vs CURD)  
(\*samples\_\*loc\_relative\_spatial\_association.png).
- CSV containing the principal component coordinates for each FOV  
(ARC1\_abundance\_FOV\_PCA.csv, ARC1\_spatial\_association\_FOV\_PCA.csv).
- CSV containing the mean fold-change in number of edges between each ASV and the corresponding p-value when compared to the null state (random spatial association matrices) (ARC1\_spatial\_enrichment\_significance.csv).

## Key takeaways

While we were not able to detect any significant microbial spatial associations based on these experiments, we think this technology has a lot of promise for generating hypotheses about microbial interactions and for understanding the context of microbes within their communities. Applying a technique to a new system is always challenging, and developing the right HiPR-FISH protocols for a new microbiome required a lot of troubleshooting by Kanvas Biosciences. There are also some inherent challenges of the technique that matter more for some sample types (in our case, dealing with lower rRNA levels in some cells), but these challenges are likely surmountable.

We're not planning to work with this data any further in the near-to-medium-term, but we encourage others to use it.

---

### Acknowledgements

Thank you to Phil Burnham and Hannah Bronson at Kanvas Biosciences for developing and executing HiPR-FISH protocols for cheese rind communities. You were fantastic collaborators!

---

# References

- 1 Borges AL, Dutton RJ, McDaniel EA, Reiter T, Weiss ECP. (2024). Paired long- and short-read metagenomics of cheese rind microbial communities at multiple time points. <https://doi.org/10.57844/ARCADIA-0ZVP-XZ86>
- 2 Shi H, Shi Q, Grodner B, Lenz JS, Zipfel WR, Brito IL, De Vlaminc I. (2020). Highly multiplexed spatial mapping of microbial communities. <https://doi.org/10.1038/s41586-020-2983-4>
- 3 Wolfe BE, Button JE, Santarelli M, Dutton RJ. (2014). Cheese Rind Communities Provide Tractable Systems for In Situ and In Vitro Studies of Microbial Diversity. <https://doi.org/10.1016/j.cell.2014.05.041>
- 4 Morin M, Pierce EC, Dutton RJ. (2018). Changes in the genetic requirements for microbial interactions with increasing community complexity. <https://doi.org/10.7554/elif.37072>
- 5 Pierce EC, Morin M, Little JC, Liu RB, Tannous J, Keller NP, Pogliano K, Wolfe BE, Sanchez LM, Dutton RJ. (2020). Bacterial–fungal interactions revealed by genome-wide analysis of bacterial mutant fitness. <https://doi.org/10.1038/s41564-020-00800-z>
- 6 Saak CC, Pierce EC, Dinh CB, Portik D, Hall R, Ashby M, Dutton RJ. (2023). Longitudinal, Multi-Platform Metagenomics Yields a High-Quality Genomic Catalog and Guides an *In Vitro* Model for Cheese Communities. <https://doi.org/10.1128/msystems.00701-22>
- 7 Li H. (2021). New strategies to improve minimap2 alignment accuracy. <https://doi.org/10.1093/bioinformatics/btab705>
- 8 Li H. (2018). Minimap2: pairwise alignment for nucleotide sequences. <https://doi.org/10.1093/bioinformatics/bty191>
- 9 Danecek P, Bonfield JK, Liddle J, Marshall J, Ohan V, Pollard MO, Whitwham A, Keane T, McCarthy SA, Davies RM, Li H. (2021). Twelve years of SAMtools and BCFtools. <https://doi.org/10.1093/gigascience/giab008>
- 10 Bonfield JK, Marshall J, Danecek P, Li H, Ohan V, Whitwham A, Keane T, Davies RM. (2021). HTSlib: C library for reading/writing high-throughput sequencing data.

<https://doi.org/10.1093/gigascience/giab007>

- 11 Altschul SF, Gish W, Miller W, Myers EW, Lipman DJ. (1990). Basic local alignment search tool. [https://doi.org/10.1016/s0022-2836\(05\)80360-2](https://doi.org/10.1016/s0022-2836(05)80360-2)
-